

Final Technical Report for Research and Development

Reference No: AOARD-08-4113

Contract No: FA2386-08-1-4113

Research term: 1 June, 2008 – 31 May, 2009

Spectroscopic Characterization of Microplasmas

September 20, 2009

Kunihide Tachibana

Professor Emeritus

Department of Electronic Science and Engineering,
Graduate School of Engineering, Kyoto University,
Kyoto-daigaku Katsura, Nishikyo-ku, Kyoto 615-8510, Japan

E-mail: tatibana@kuee.kyoto-u.ac.jp

Report Documentation Page				Form Approved OMB No. 0704-0188	
Public reporting burden for the collection of information is estimated to average 1 hour per response, including the time for reviewing instructions, searching existing data sources, gathering and maintaining the data needed, and completing and reviewing the collection of information. Send comments regarding this burden estimate or any other aspect of this collection of information, including suggestions for reducing this burden, to Washington Headquarters Services, Directorate for Information Operations and Reports, 1215 Jefferson Davis Highway, Suite 1204, Arlington VA 22202-4302. Respondents should be aware that notwithstanding any other provision of law, no person shall be subject to a penalty for failing to comply with a collection of information if it does not display a currently valid OMB control number.					
1. REPORT DATE 29 SEP 2009		2. REPORT TYPE		3. DATES COVERED	
4. TITLE AND SUBTITLE Spectroscopic Characterization of Microplasmas-Phase III				5a. CONTRACT NUMBER FA23860814113	
				5b. GRANT NUMBER	
				5c. PROGRAM ELEMENT NUMBER	
6. AUTHOR(S) Kunihide Tachibana				5d. PROJECT NUMBER	
				5e. TASK NUMBER	
				5f. WORK UNIT NUMBER	
7. PERFORMING ORGANIZATION NAME(S) AND ADDRESS(ES) Kyoto University,Kyoto-Daigaku Katsura, Nishikyo-ku,Kyoto 615-8510,Japan,NA,NA				8. PERFORMING ORGANIZATION REPORT NUMBER N/A	
9. SPONSORING/MONITORING AGENCY NAME(S) AND ADDRESS(ES)				10. SPONSOR/MONITOR'S ACRONYM(S)	
				11. SPONSOR/MONITOR'S REPORT NUMBER(S)	
12. DISTRIBUTION/AVAILABILITY STATEMENT Approved for public release; distribution unlimited.					
13. SUPPLEMENTARY NOTES					
14. ABSTRACT In this study, a new design for a unit discharge cell has been developed. It has a floating electrode in the well of the top electrode above the bottom electrode, in which the bright spot can be spatially fixed irrespective of the applied voltage phases. As an evidence of a new function driven from integrated structure, a frequency-dependent deformation phenomenon of mm-wave transmittance through a perforated metal-plate filled with microplasmas was observed. Also investigated discharge plasmas generated in artificial media: liquids with injected bubbles or atmospheric gases with mists of &#956;m to nm order sizes. As a trial, a fabric-type electrode assembly dipped in aqueous solution of electrolyte was used and the discharge phenomenon in bubbles generated by electrolysis using optical emission spectroscopy was studied. The plasma emission spectrum in the discharge in bubbled water with a point-to-plane electrode configuration was observed and widely broadened line spectra of hydrogen atoms were measured. A study on the discharge in air with liquid mists has been tested as well with the developed mesh-electrode configuration with preliminary results.					
15. SUBJECT TERMS					
16. SECURITY CLASSIFICATION OF:			17. LIMITATION OF ABSTRACT	18. NUMBER OF PAGES 19	19a. NAME OF RESPONSIBLE PERSON
a. REPORT unclassified	b. ABSTRACT unclassified	c. THIS PAGE unclassified			

Abstract

In the 3rd year of this joint research project, we continued the preceding two-years' study on the properties of a single microplasma jet driven by a low frequency power source in atmospheric pressure He gas flow. For the deeper mechanistic understandings of a thin and long plume effused into air along the gas flow, we employed two laser spectroscopic techniques: a laser induced-fluorescence method for N_2^+ ions and a laser absorption method for metastable He^* atoms. The measured spatiotemporal behaviors show noticeable differences between the situations with and without the conductive substrate in the downstream. Without the substrate the plasma plume propagated like a streamer in a positive corona discharge in the positive phase of applied voltage. On the other hand, when the substrate was placed at a finite distance the propagation speed enhanced, and as soon as the streamer head reaches the substrate the second discharge followed like in a dielectric barrier discharge (DBD). We have also developed a CO_2 laser heterodyne interferometer for the measurement of electron density n_e in microplasmas with a spatial resolution better than 100 μm . We performed the measurement in a pulsed DC microplasma jet with a micro hollow-cathode configuration and successfully derived the radial profile of n_e across a plasma jet plume of about 1 mm diameter. As an application of the microplasma jet, we have been working on the deposition of SiO_2 films, and realized a high-rate deposition by using tetra-ethoxy-silane (TEOS) as the source material. In this year, we challenged to the deposition of ZnO films with bis(octane-2,4-dionato)zinc ($\text{Zn}(\text{OD})_2$) source, and succeeded in the deposition of transparent film at a deposition rate of a few tens of nm/s with heated substrates at 250°C.

In the second part of this research project, we have been working on microplasma integrated devices. We developed a new design for a unit discharge cell. It has a floating electrode in the well of the top electrode above the bottom electrode, in which the bright spot can be spatially fixed irrespective of the applied voltage phases. As an evidence of a new function driven from integrated structure, we observed a frequency-dependent deformation phenomenon of mm-wave transmittance through a perforated metal-plate filled with microplasmas. We have also been investigating discharge plasmas generated in artificial media: liquids with injected bubbles or atmospheric gases with mists of μm to nm order sizes. As a trial, we used a fabric-type electrode assembly dipped in aqueous solution of electrolyte and studied the discharge phenomenon in bubbles generated by electrolysis using optical emission spectroscopy. We also observed the plasma emission spectrum in the discharge in bubbled water with a point-to-plane electrode configuration and measured widely broadened line spectra of hydrogen atoms. A study on the discharge in air with liquid mists has been tested as well with our developed mesh-electrode configuration with preliminary results.

1. Introduction

In recent years, microscale plasmas of μm to mm ranges have been attracting much scientific and technological attention. Those microplasmas generally operated at high pressure regions including atmospheric pressure exhibit characteristics that differ from traditional plasmas operated at lower pressure regions in their plasma parameters and other parameters originating from their small dimensions. Actually, the electron density n_e of typical microplasma lies in the range of 10^{12} to 10^{16} cm^{-3} even though the ionization degree is rather small. As for the electron temperature T_e , it shows non-equilibrium natures inherently due to the short residence time in small space or short duration of pulsed discharge in the generation. When those characteristics are well combined with the inherent properties of plasmas as reactive, light-emissive and conductive/dielectric media, there appear a variety of potential applications for new tools of material syntheses, micromachining, micro chemical analyses as well as photonic devices. In the study of this joint research, by using various spectroscopic techniques, we have been characterizing the basic plasma properties of microplasmas in two different types: isolated microplasma devices and large scale microplasma-integrated devices, aiming at applications for material processing and controlling electromagnetic waves. The kinds of gases of our major interest are rare-gases such as He, Ne, and Ar, which are admixed with compositions of ambient air such as N_2 , O_2 , and H_2O for the formation of reactive species in material processing applications. We have also been trying to use liquids with bubbles or gases with mists as new artificial media for the generation of microplasmas.

2. Experimental Results

2.1. Single microplasma sources

2.1.1. Diagnostics of microplasma jets

(a) Laser spectroscopic measurements

First, we measured the spatiotemporal distribution of metastable $\text{He}^*(^3\text{S}_1)$ atoms in the plasma plume by diode laser absorption spectroscopy (LAS) at the 1083 nm transition with the experimental configuration shown in **Fig. 1(a)**. The inner diameter of the glass capillary was 4 mm and He gas was fed through the bore at a flow rate of 2.8 L/min. The driving bipolar impulse-voltage waveform is shown in **Fig. 1(b)**. We used a typical frequency of 5 kHz in most of our measurements. The two-dimensional projection image of the He^* density distribution was obtained from the line-integrated absorption signal by scanning the radial and axial positions of the laser beam. From the result shown in **Fig. 2** the density of non-charged He^* atoms looks like propagating forward as a bullet at an approximate speed of 50 km/s. This is consistent with the previous CCD camera observation and laser induced fluorescence

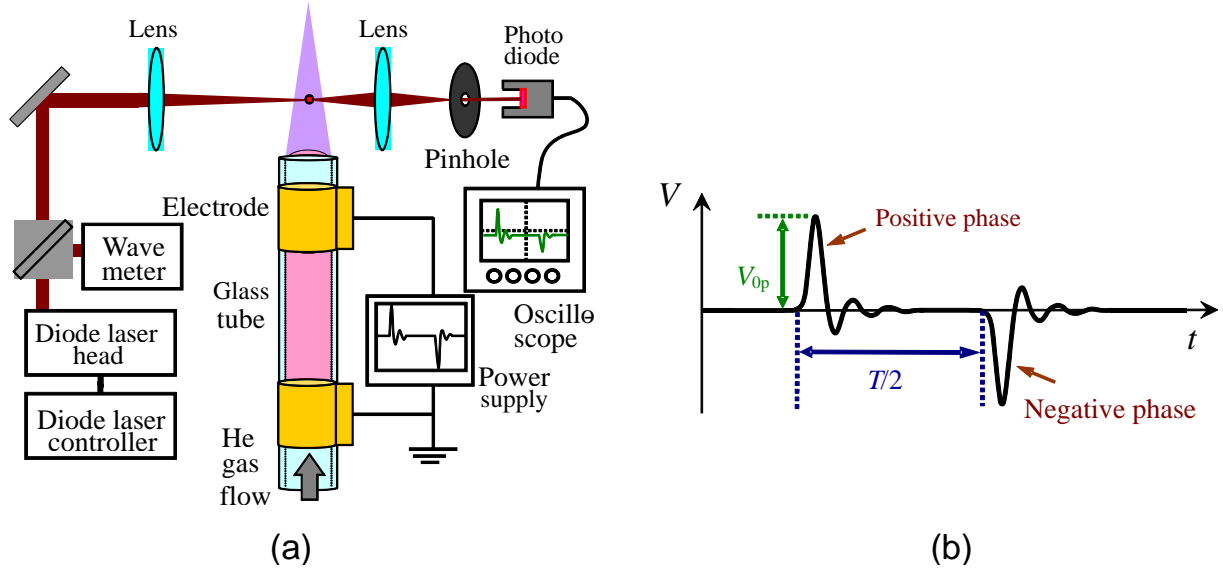


Fig. 1 (a) Experimental setup of plasma jet with laser absorption measurement apparatus and (b) driving voltage waveform.

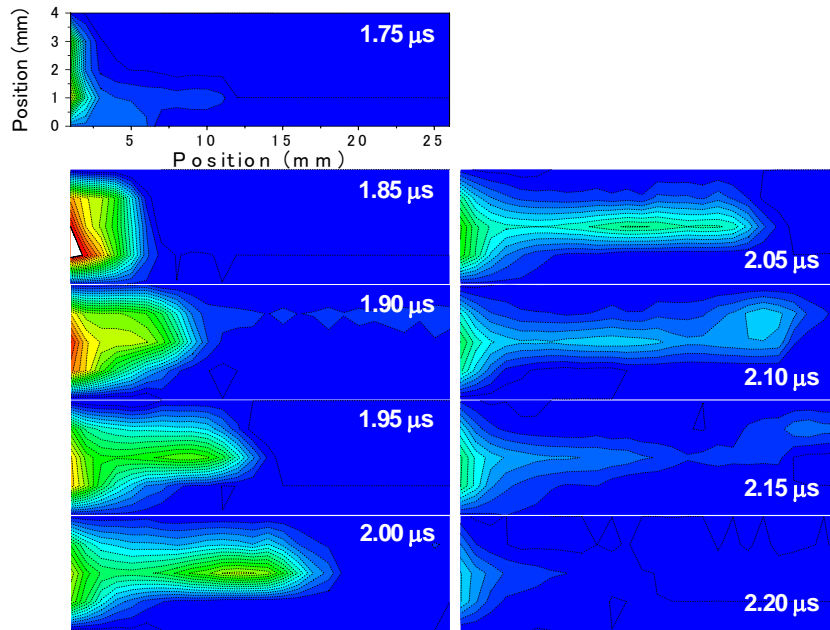


Fig.2 Spatiotemporal distribution of metastable He* atoms measured by LAS.

measurement of N_2^+ ions, and proves that the production front of excited atoms and also charged particles is moving like a streamer head in a corona discharge.

When we set a conductive substrate at a distance of 20 mm from the nozzle exit, the appearance of the spatiotemporal distribution differs dramatically. **Figures 3** show the He* atom density distributions in the axial position vs. time domain in (a) positive phase and (b) negative phase of the applied voltage. In the positive phase, it is seen that a weaker streamer

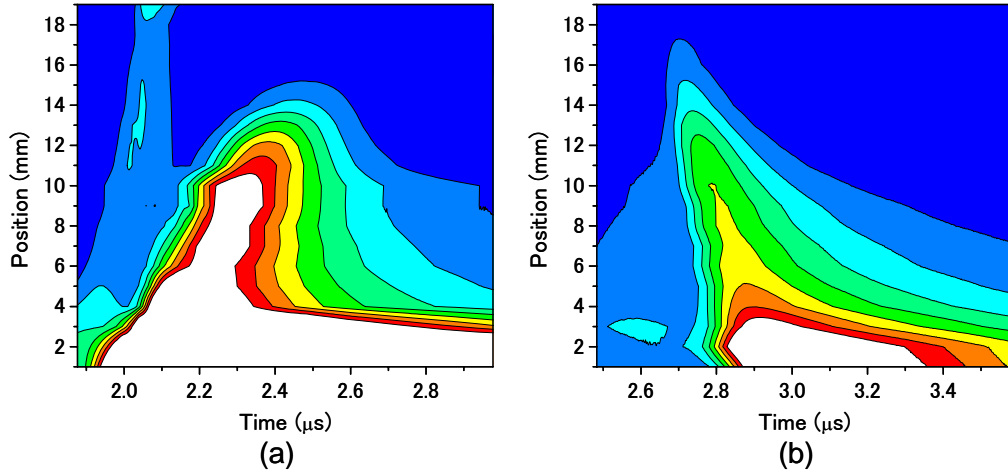


Fig. 3 Spatiotemporal distribution of metastable He^* atoms in between the nozzle exit (at $z = 0$ mm) and grounded substrate (at $z = 20$ mm) at (a) positive and (b) negative phases of the applied voltage.

propagates toward the grounded substrate (tentative cathode) at a very fast speed of about 120 km/s and the second streamer follows with much stronger intensity leaving the high density region near the exit of the nozzle. This is similar to the typical behavior seen in a DBD scheme with a narrow gap. The acceleration of the first streamer is due to a larger electric field formed between the really existing electrodes. In the negative phase, however, the discharge looks like to propagate backward from the substrate toward the exit of the nozzle.

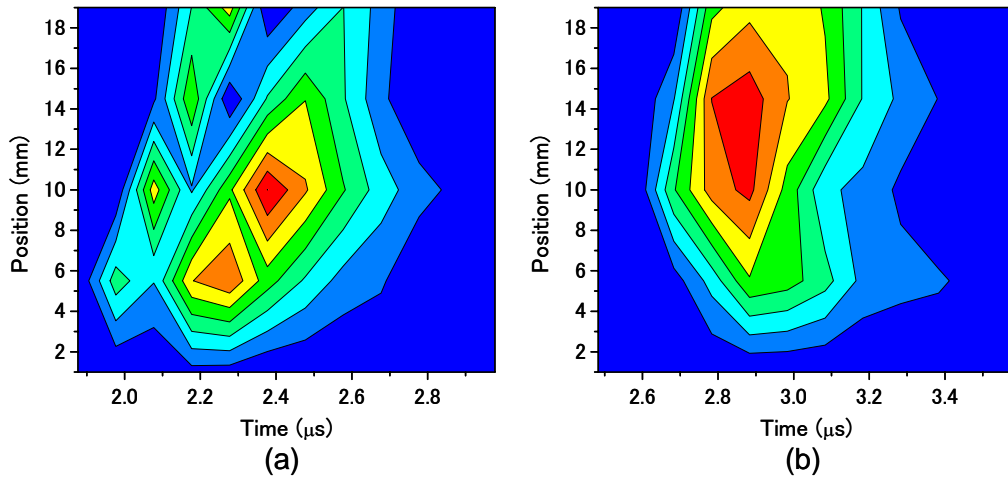


Fig. 4 Spatiotemporal distribution of N_2^+ ions measured by LIF atoms in between the nozzle exit and grounded substrate at (a) positive and (b) negative phases of the applied voltage in the same situation in Fig. 3.

The spatiotemporal distributions of N_2^+ ions measured by laser induced fluorescence (LIF) spectroscopy in the same situations as above are shown in **Fig. 4** for (a) positive and (b) negative phases, respectively. The behavior in the positive phase is similar to that of He^* atoms in Fig. 3(a) on the whole except the density peaks in the middle and not at the nozzle exit. It is simply due to the concentration of N_2 molecules supplied by the diffusion of ambient air, which is much less at the exit of the He gas flow. In the negative phase, it is seen that the N_2^+ ion density rises simultaneously within the gap space. If we take a closer look at the result in Fig. 3(b), the rising edge of He^* atom density looks like almost vertical with time in consistent with the behavior of N_2^+ ions in Fig. 4(b). The shift in the peak of He^* atoms near the nozzle exit may be attributed to the accumulation of the density with time due to the longer lifetime of the metastable atoms in purer He ambient.

Figure 5 (a) shows the radial distributions of He^* atom density in the positive and negative phases measured at 5 mm distance from the nozzle exit with the presence of the conductive substrate. (See Ref. 31 for the detailed procedure of derivation of the radial profile.) A characteristic difference is seen between them; the distribution takes a hollow shape in the positive phase while it takes a center-peaked shape in the negative phase. It is due to difference in the nature of negative and positive corona discharge modes. The distribution of N_2^+ ions in the positive phase is shown in Fig. 5(b) which is similar to that of He^* atoms.

Figure 6 shows the normalized emission intensities of the 2nd positive band (SPB) of N_2^* at 337 nm and the 1st negative band (FNB) of N_2^+ at 391 nm measured as a function of time at 1 mm from the substrate surface; (a) and (b) correspond to the positive and negative phases, respectively. The densities of metastable He^* atoms and N_2^+ ions measured by LAS and LIF methods are also plotted together. It is seen that only the first sharp peak appears in the

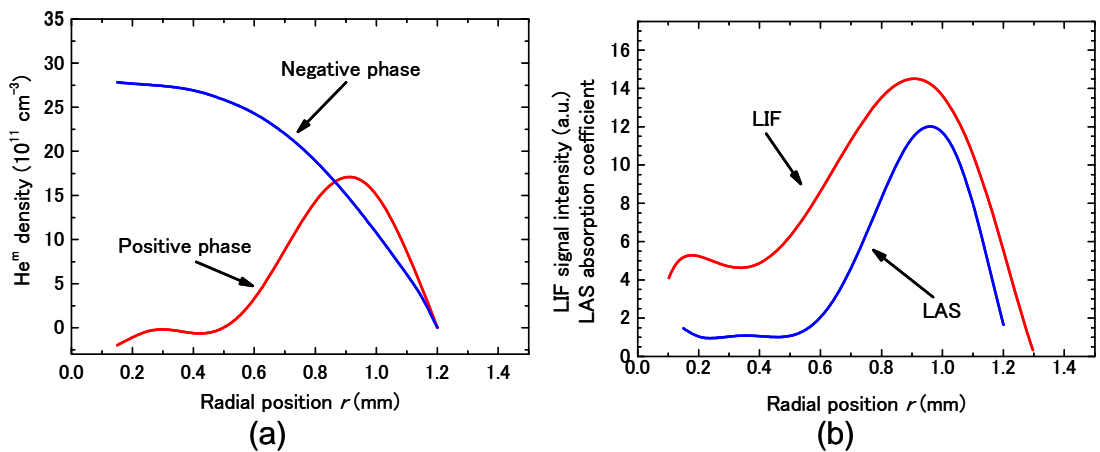


Fig. 5 (a) Radial profile of metastable He^* atom density in positive and negative phases, and (b) He^* atom density and N_2^+ ion density in positive phase measured at 5mm from the exit.

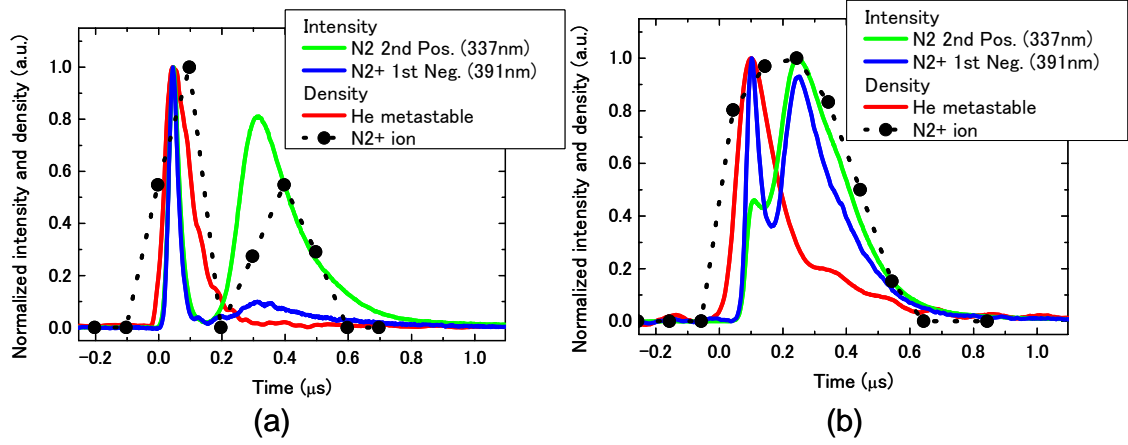


Fig. 6 Emission intensities of $N_2^* 2^{\text{nd}}$ positive band and $N_2^+ 1^{\text{st}}$ negative band together with densities of metastable He^* atoms and N_2^+ ions measured in (a) positive and (b) negative phases at 1mm distance from substrate.

density of metastable He^* atoms, but the broad and strong second peak appear in the SPB emission and the density of N_2^+ ions. This suggests that the ionization mechanism in the second streamer discharge is predominated by the direct electron impact ionization of N_2 rather than the Penning ionization with He^* atoms.

(b) Laser interferometric measurements

For the measurement of spatiotemporally resolved electron density n_e in a microplasma jet, we have developed a laser heterodyne interferometer using a CO_2 laser of $10.6 \mu\text{m}$ wavelength as the light source as shown schematically in **Fig. 7**. The laser beam was

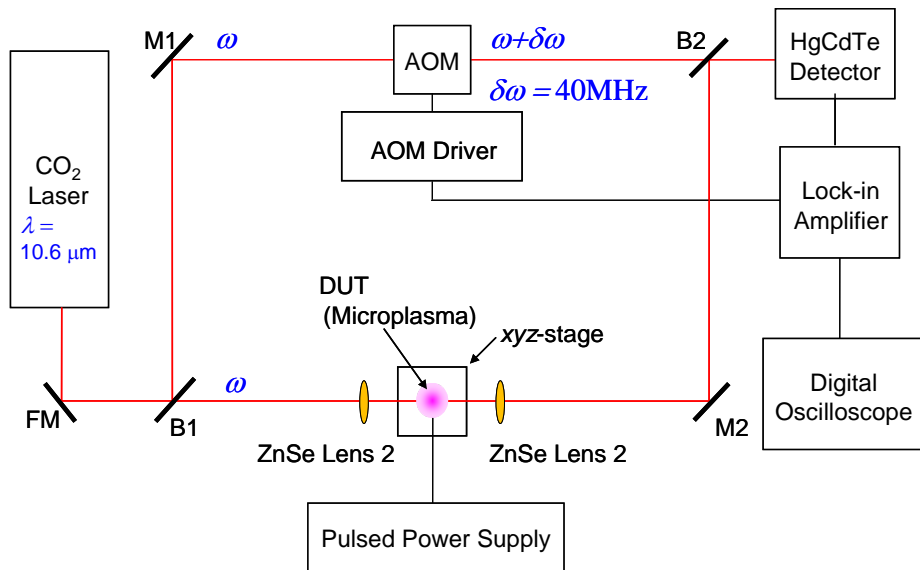


Fig. 7 Experimental setup for CO_2 laser heterodyne interferometry.

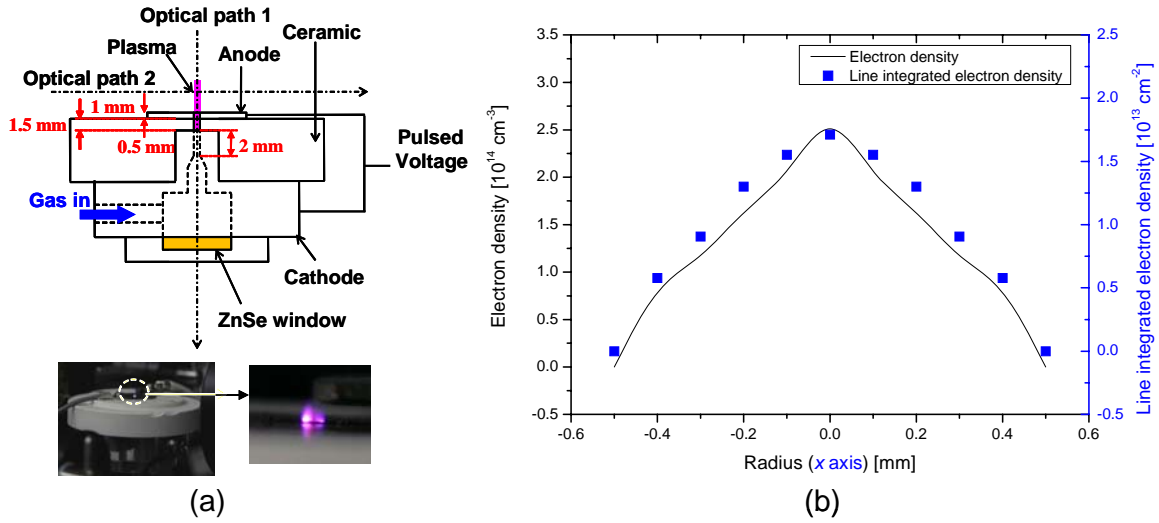


Fig. 8 (a) Scheme of micro hollow-cathode discharge device and (b) measured radial profile of ne using CO₂ laser heterodyne interferometry.

modulated by an acoustoptic modulator (AOM) at a frequency of 40 MHz, and the phase shift caused by the presence of microplasma was detected at the frequency by a lock-in amplifier. The signal was averaged many times by a digital oscilloscope to derive a small phase shift component on the order of 0.01 degree. As the microplasma jet (Device Under Test: DUT), we used a DC discharge hollow cathode device as shown in **Fig. 8** (a), which was pulse modulated in order to separate the electron-density contribution from the gas-density-change contribution by using their different temporal behaviors. (See [Ref. 28](#) for the details.) Figure 8(b) shows the measured radial profile of n_e in the microplasma jet at a distance of 1 mm from the exit. The measured line integrated density (along the line-of-sight) data were Abel inverted to derive the final radial distribution. The peak density was about $2.5 \times 10^{12} \text{ cm}^{-3}$ at a current of 120 mA when atmospheric pressure He gas was fed at a flow rate of 6 L/min.

2.1.2 Applications

(a) Microplasma enhanced CVD of SiO₂ films

We have been working on the deposition of SiO₂ films by using the LF-driven microplasma jet with vaporized tetra-ethoxy-silane (TEOS) as the source material. In a crossed configuration of the plasma jet with the source flow at the substrate surface, we attained a very high deposition rate of a few hundreds of nm/s on a Si substrate with the aid of ozone mixing. However, it was found that the deposition rate decreased on a SiO₂/Si substrate as shown in **Fig. 9** (a), and more drastically on a glass substrate. Even on a Si substrate the deposition rate decreased as the deposited film thickness increased with the deposition time.

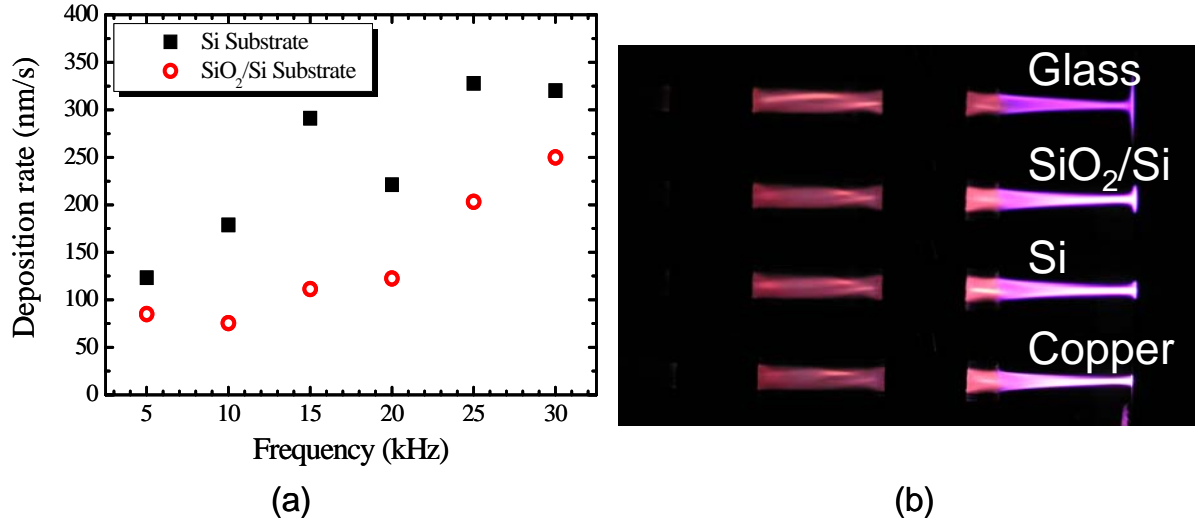


Fig. 9 (a) Deposition rate of SiO₂ film on Si and SiO₂/Si substrates and (b) difference in the appearance of plasma plume with different kinds of substrates.

In order to investigate this effect, we observed the differences in the plasma plume with several kinds of substrates. The results are shown in Fig. 9 (b). It was seen that at the surface of a glass substrate, the plume split along the surface and the whole emission intensity was weaker. The tendency became smaller as we used a SiO₂/Si substrate. With conductive substrates such as Si and copper the tip of the plume does not spread and the emission intensity of the plume became stronger. This can be attributed to the accumulated charge on the substrate surface which tends to repel the plasma plume. The accumulated charge density depends on the capacitance, i.e., a larger tolerance toward the plasma exposure is allowed at a larger capacitance. Since the capacitance decreases as the deposited SiO₂ film thickness

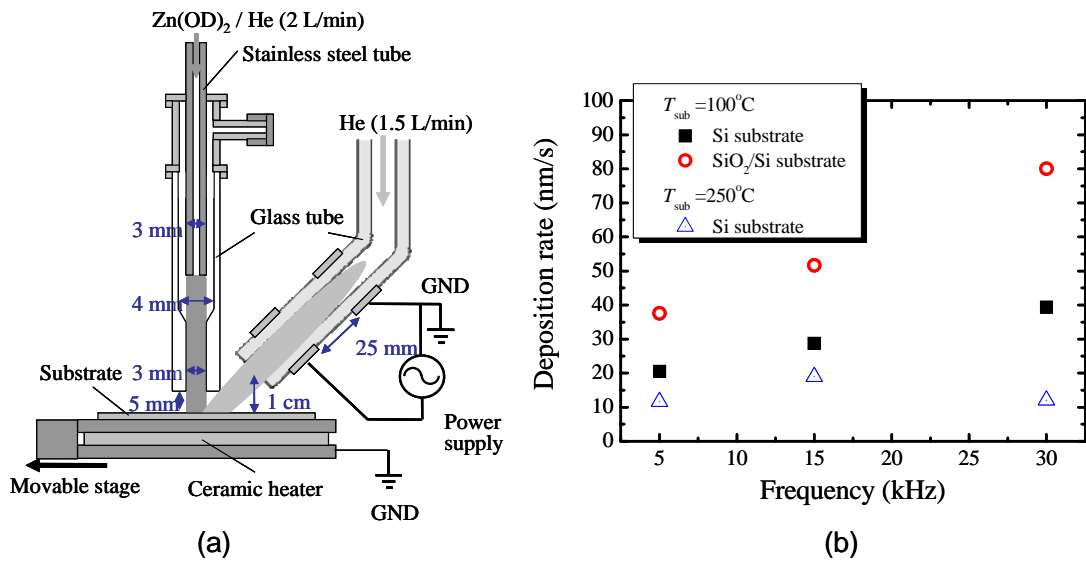


Fig. 10 (a) Experimental setup for ZnO deposition and (b) obtained deposition rate.

increases, the plume tends to spread more and the deposition rate decreases (see [Ref. 32](#)).

(b) Microplasma enhanced CVD of ZnO films

This year we started to deposit ZnO films using bis(octane-2,4-dionato)zinc (Zn(OD)_2) source as the source material. We used also the crossed configuration as shown in **Fig. 10** (a). The obtained deposition rate is shown in **Fig. 10** (b) at two substrate temperatures: 100°C and 250°C. Although the deposition rate is higher at 100°C, the deposited film consists mostly of residual source material which are not fully decomposed. At the elevated temperature of 250°C the deposited film became transparent and the concentration of carbon bonds was much less as characterized by XPS and FT-IR spectroscopy as shown in **Fig. 11**. However, we have to improve the conductivity further by using appropriate post-deposition treatments.

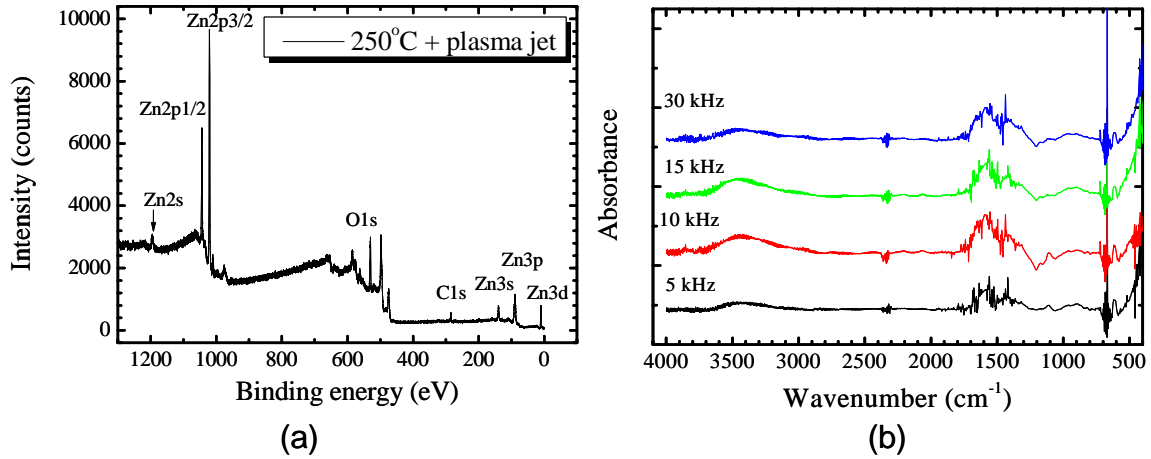


Fig. 11 (a) XPS spectra and (b) FT-IR spectra measured on ZnO films deposited on Si substrate at 250°C with different driving frequency of microplasma jet.

2.2. Integrated Microplasma Devices

2.2.1. New design of microdischarge cell

We have designed a new structure of unit microdischarge cell, which has coaxial electrode structure with a square floating electrode within the well of the top electrode, being stacked on the dielectric barrier over the bottom electrode as shown in **Fig. 12**. Both the top electrode and the floating electrode were covered by dielectric material to prevent the ion sputtering. We prepared two sets of different sizes D as shown in the figure (see [Ref. 26](#)).

The spatiotemporal behaviors of optical emission from excited Ne atoms are shown in **Fig. 13** at several values of the filling gas pressure p . The corresponding cross sectional profiles are shown in **Fig. 14** at several timings designated in **Fig. 13** with Roman numerals. It is very interesting to see that the discharge mode changes as the pressure decreases toward the

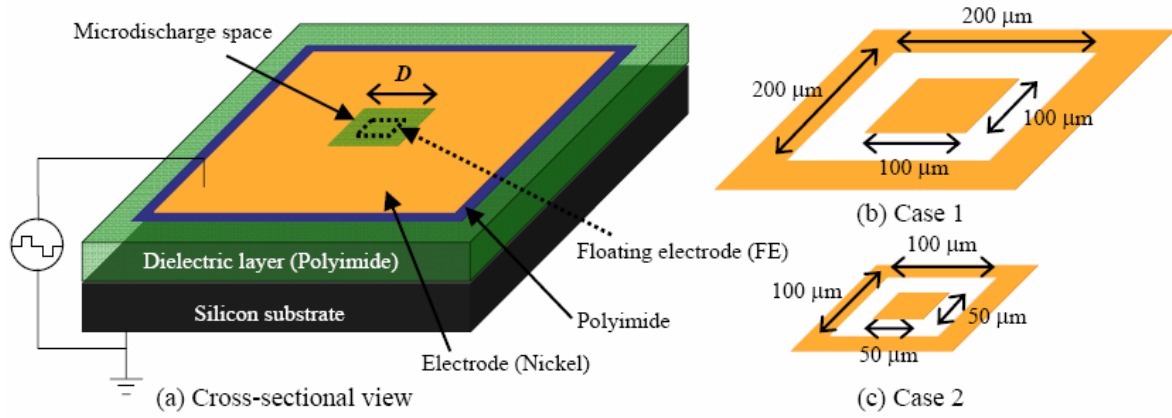


Fig. 12 Microdischarge cell of coaxial electrode structure with a floating electrode.

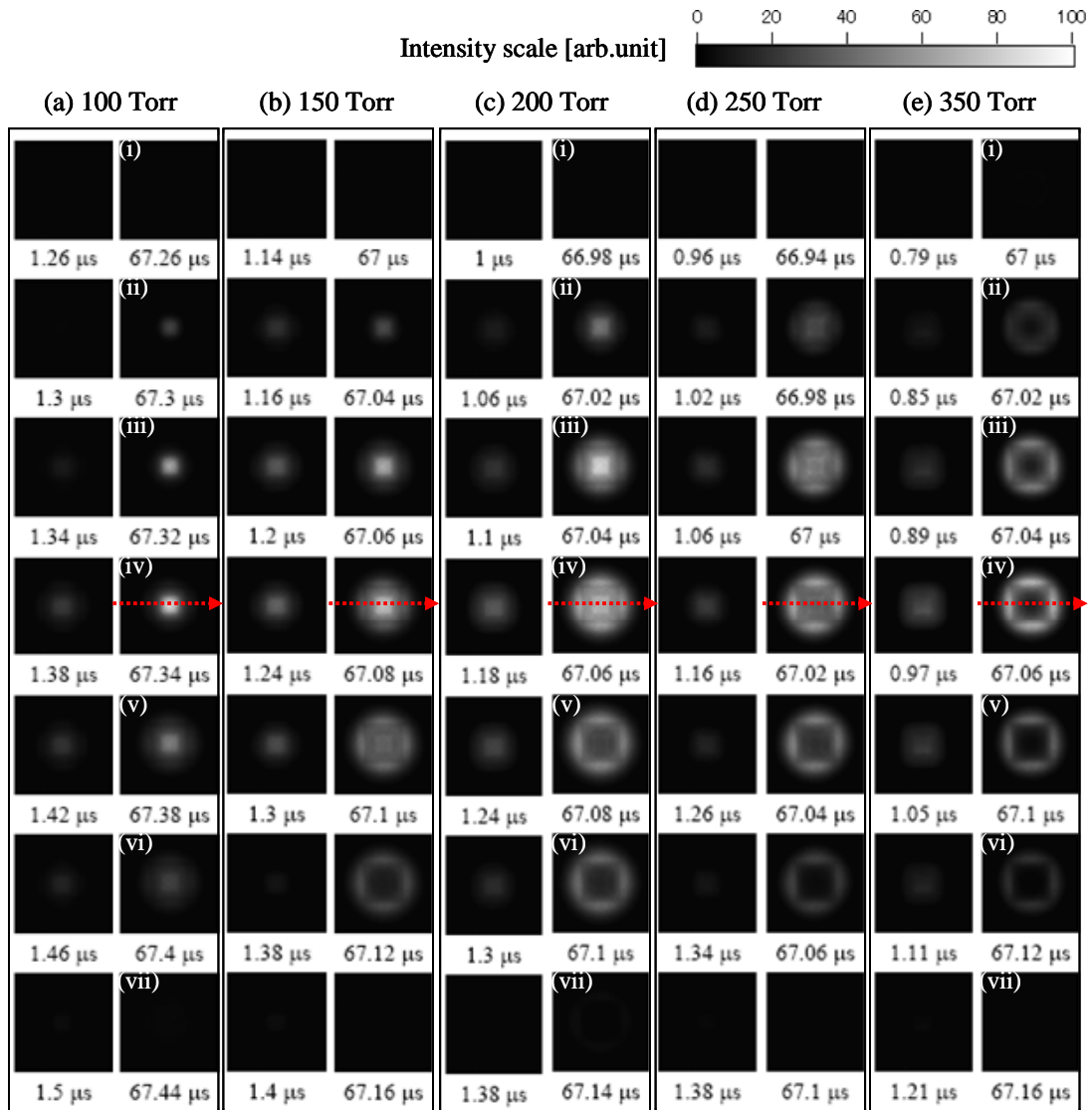


Fig. 13 Spatiotemporal behavior of optical emission in a coaxial microdischarge cell filled with Ne at several values of gas pressure.

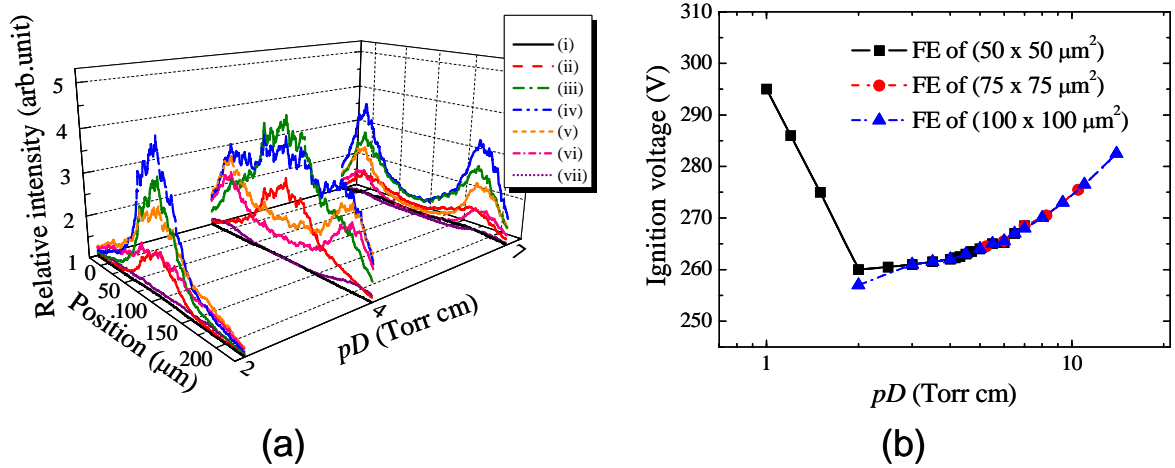


Fig. 14 (a) Cross sectional intensity profiles along the center line at several timings indicated in Fig. 13 and (b) curves of ignition voltage vs. pD value (Paschen curve).

Paschen minimum as shown in Fig. 14 (b). That is to say, the bright spot tends to stay always on the floating electrode irrespective of the polarities of the applied voltages between the bottom and outer electrodes. As the possible mechanisms for these observed discharge phenomena, the intensified electric field on and around the aperture leads to localized ionization at relatively low pressure, and a strong nonlinear tendency in the ionization coefficient α as a function of the reduced electric field E/p affects the pD value at the transition (see Ref.30). The formation of the cathode fall within the discharge space, whose length becomes longer as p decreases, also affects the transition. However, more quantitative investigation is necessary for the full explanation of the mechanisms. In any case, this newly found operation mode may be favorable if this structure is applied to a unit cell of a PDP.

2.2.2. Plasma metamaterial

We have been trying to derive new functions from periodic arrays of microplasmas, and realized the concept of plasma photonic crystals as reported previously. At the moment we are working on the creation of metamaterials with spatially modulated material's constants, i.e., permeability μ , permittivity ϵ and conductivity σ , at a pitch (or lattice constant) less than the wavelength of electromagnetic waves propagating through the medium. As such an example, we are using metal plates with two-dimensional hole arrays (just like punched metal plates). The periodically perforated structure itself is known to have a metamaterial nature. What we aim at with this structure is to deform the anomalous frequency response of this structure dynamically with and without the microplasmas filling the holes. The actual structure used in the experiment is shown in Fig. 15 (a). Microplasmas are generated in a DBD scheme by applying pulsed voltage between the insulator coated metal plates. Electromagnetic waves in

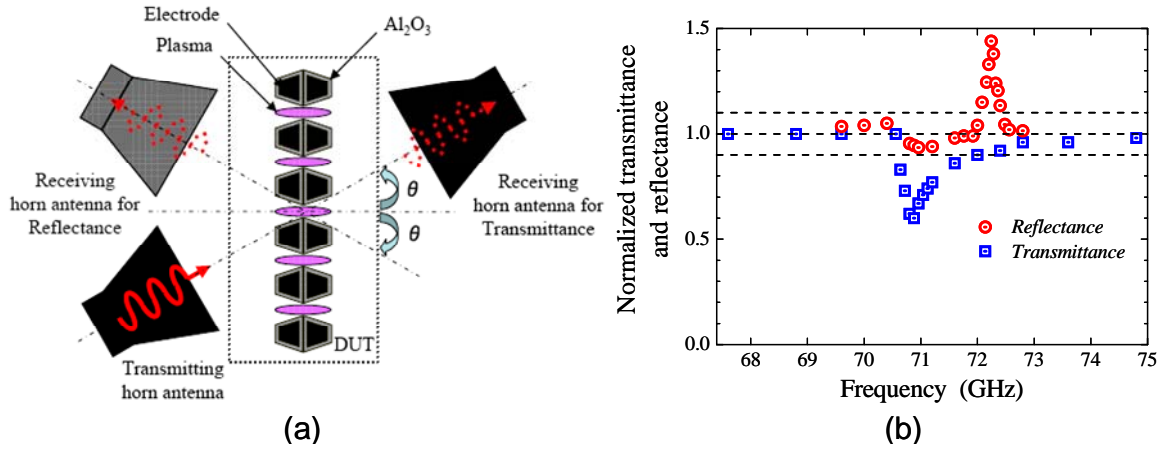


Fig. 15 (a) Experimental setup and (b) the results of normalized transmittance and reflectance components measured as a function of frequency.

millimeter wavelength range were transmitted by a horn antenna at an incident angle of $\theta = 18^\circ$ or 30° . The transmittance component was received by the second horn antenna on the other side of the electrode structure, while the reflectance component was observed by the third antenna placed on the same side.

Figure 15 (b) shows the normalized transmittance and reflectance signals (signal ratios with and without microplasmas) measured at $\theta = 18^\circ$ as a function of frequency. Unusual responses of electromagnetic waves due to the generation of microplasmas appeared in the narrow frequency range from 70 to 73 GHz. The transmittance was suppressed up to 40% and the reflectance was enhanced up to 45% of their initial values. The shifts of these peak frequencies from the resonance frequency of inherent spoof surface plasmons of the perforated metal plates can be attributed to the presence of microplasmas with lower permittivity than 1. (See [Ref. 27](#) for more detailed arguments.)

2.3. Microplasma generation in artificial media

2.3.1. Discharge in bubbles generated by electrolysis

As the first example of the discharge in artificial media, we tried to make discharge in underwater micro bubbles produced by electrolysis with addition of Na_2CO_3 (3 wt %). The experimental apparatus is schematically shown in **Fig. 16** (a) and (b). The electrode had a fabric structure with an insulated metal wire as the warp and a bare metal wire as the weft. The electrode was separated from the third electrode with a distance of a few cm and those electrodes were connected with a DC power supply for the electrolysis. The generated bubbles were held on the surface of the fabric electrode. By applying AC voltage of about 3 kV p-p, the discharge was recognized to occur inside the micro bubbles. The figure of merit in

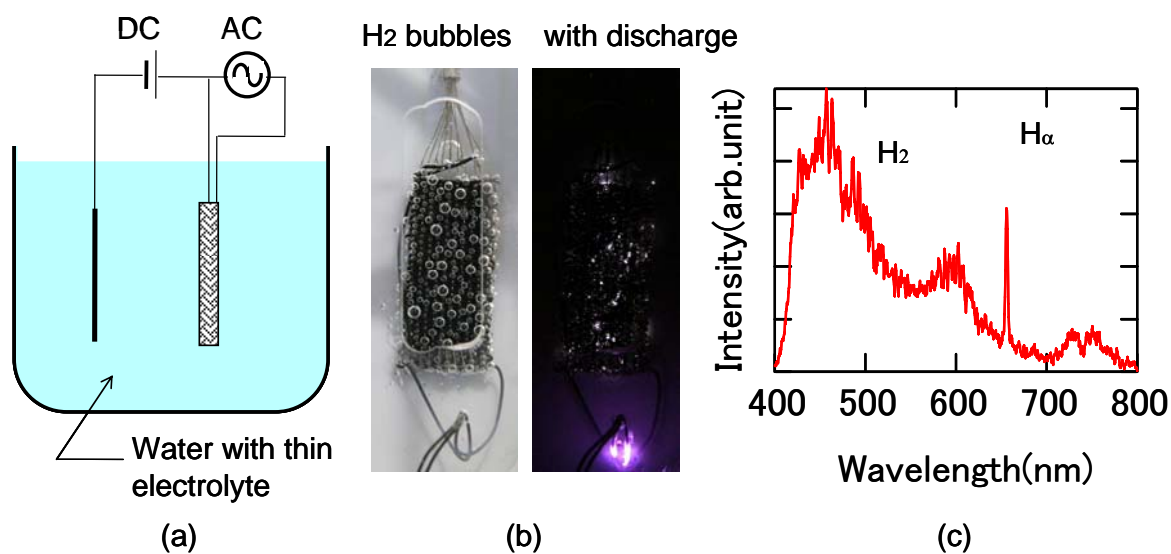


Fig. 16 (a) Scheme of experimental set up and (b) electrode assembly with micro bubbles produced by electrolysis and the discharge image.

this configuration is explained as follows; the electrode structure not only allows low-voltage ignition of the atmospheric pressure discharge in hydrogen or oxygen containing micro bubbles but also works effectively in producing and holding bubbles on its surface. The generation of reactive species was verified by optical emission from the produced microplasmas as shown in Fig 16 (c), and their transport into the solution was monitored by the change in pH value (see [Ref. 25](#)).

In order to make this system more practical for such an application to the sterilization and purification of water, a dynamic cycle should be established for the bubble generation, the microdischarge generation and the release of active species into solution by breaking bubbles with discharge or forced liquid flow.

2.3.2. Discharge in bubbled water

As the second example, we introduced micro air bubbles into water and tried to make discharge in the mixture. We used an open-end insulated wire as the anode and a metal plate placed at the bottom of the vessel as the cathode. The variation in the appearance of the discharge was shown in **Fig. 17** (a) with different bubble concentration. The measured ignition and sustain voltages with and without bubbles at a certain concentration is plotted in Fig. 17 (b) as a function of the discharge repetition frequency. It is seen that both the ignition and sustain voltages in the bubbled water are much lower than those in the pristine water. The decreasing tendency seen in the bubbled water with the increase of the repetition frequency is attributed to the generation of bubbles by discharge itself.

However, the situation shown here is not fit to the category of artificial media as yet since

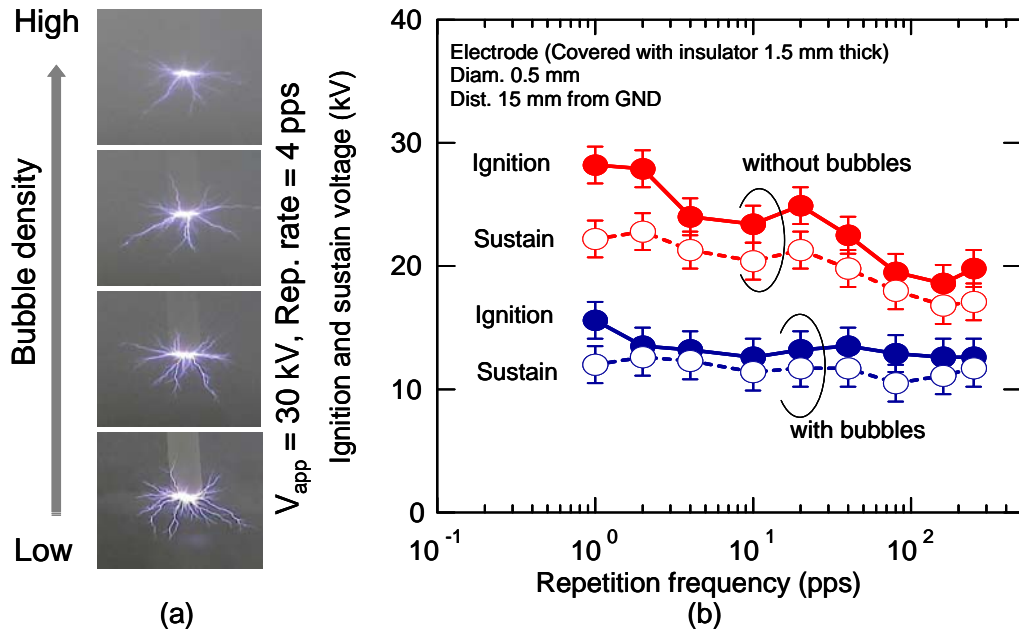


Fig. 17 Discharge image in bubbled water and the ignition and sustain voltages as a function of discharge repetition.

the bubbles are not introduced under controlled conditions and, moreover, the size and the density of bubbles are not specified as yet. We are now preparing to measure those parameters by using a dynamic light scattering method. Introduction of other gases than air is also under

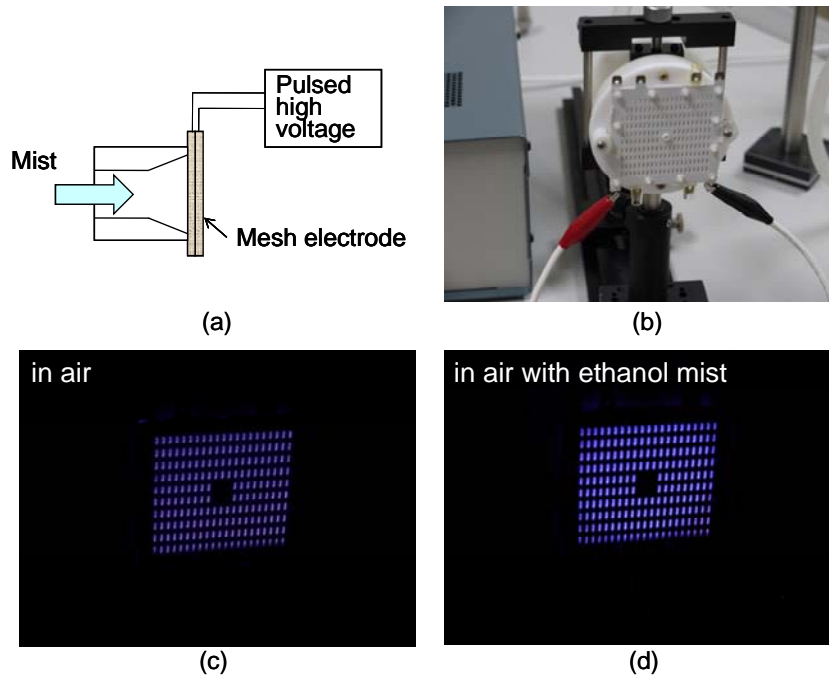


Fig. 18 (a) Scheme and (b) photo of discharge device together with discharge images in (c) air and (d) air containing ethanol mist.

future planning.

2.3.3. Discharge in misted air

As the third artificial media, we tried to use air including micro scale liquid particles (mist). The mist was generated by an ultrasonic vibrator and transported to the discharge device with the carrier gas (N_2). We used the same stacked mesh electrode as used in the experiment described above in section 2.2.2. The experimental setup and the discharge images without and with ethanol mist injection are shown in **Fig. 18**. It is noticed that the color changes into whitish blue with mist injection, and the discharge operation is kept stable. In future, we plan to apply this device for environmental or biomedical applications.

3. Summary and Conclusions

In this year, we have firstly performed systematic spatiotemporal measurements of metastable He^* and N_2^+ ions for understanding the propagation mechanisms of plasma plume in a LF-driven microplasma jet. Especially, the effect of a substrate placed in front of the jet was investigated for the propagation of plasma jet and the deposition of SiO_2 and ZnO films caused by the accumulated charges on the surface. As for the diagnostics of the electron density n_e in a microplasma jet, we applied the CO_2 -laser heterodyne interferometer which we had developed last year to a micro hollow cathode device. The radial distribution of n_e across the plasma jet was successfully measured with a spatial resolution of 100 μm .

Secondly, we have worked on integrated microplasma devices. As a new design of a unit discharge cell, we developed a coaxial structure with a floating electrode in the well of the top electrode. We observed a discharge mode transition in the pressure range near the Paschen minimum, where the bright spot of the discharge stays steadily over the floating electrode in both phases of the polarity of applied voltage. Based on this finding, we plan to apply this structure to photonic devices such as a flat-panel light source etc. We have also been working on the derivation of new functions from arrays of microplasmas. This year, we tested a perforated metal plate structure for modifying the propagation characteristics of electromagnetic waves through the structure. We observed sharp resonances of the transmittance and the reflectance components in the narrow frequency range of electromagnetic waves caused by the presence of microplasmas filling the holes.

Thirdly, we have done a series of preliminary work on the microplasma generation in artificial media composed of mixtures of gases and liquids. As an example, we tried the underwater discharge in bubbles generated by electrolysis in aqueous solution of electrolyte. The successful generation of microdischarge in hydrogen or oxygen bubbles was verified by optical emission spectroscopy. Another example we tried was the discharge in bubbled water, where we injected micro bubbles into circulating water. We observed a large decrease in the

firing voltage with the forced injection of bubbles. For more quantitative study, we are preparing an *in situ* dynamic light scattering method. As a complementary concept, we have been studying the discharge in misted air. We tried to generate micro scale liquid particles by an ultrasonic vibrator and transport the mist into the mesh-type discharge device, where we observed the color change in the discharge due to the evaporated mist. We have to continue this work for more detailed characterization of the device performance.

In conclusion, we have studied on the characterization of microplasmas in both single uses and integrated uses by using various spectroscopic methods. The most remarkable outcome is the clarification of the propagation mechanisms of plasma plumes in a LF-driven microplasma jet. Through this project we have learned a lot on the new structures of microplasma devices and new functions derived from their integrations. Hereafter, we will still continue our diagnostic work and also look for suitable applications of microplasma devices in environmental and biomedical areas under well characterized conditions.

4. Presentations and Publications

4.1. Presentations

1. K. Tachibana: “*Creation of Nobel Electromagnetic and Reactive Media from Microplasmas* (Invited)”, 3rd International School of Advanced Plasma Technology (Varenna, Italy, Jul. 2008).
2. Y. Ito, K. Urabe, N. Takano and K. Tachibana: “*Diagnostics of Low-frequency Plasma Jet and Its Application to Deposition of Silicon Dioxide Films*”, 3rd International School of Advanced Plasma Technology (Varenna, Italy, Jul. 2008).
3. K. Tachibana: “*Microplasma Sources and Their Applications to Material Processing* (Invited)”, 1st International Conference on Microelectronics and Plasma Technology (ICMAPS 2008), (Jeju, Korea, Aug. 2008).
4. O. Sakai, T. Shimomura, D.-S Lee and K. Tachibana: “*Design and Verification of Metamaterials Composed of Microplasmas*”, 2nd International Congress on Advanced Electromagnetic Materials in Microwaves and Optics (Metamaterials '08) (Pamplona, Spain, Sep. 2008).
5. T. Naito, O. Sakai and K. Tachibana: “*Electromagnetic Properties in a Plasma Photonic Crystal and Its Dispersion Relation in Complex Wave Number Space*”, 2nd International Congress on Advanced Electromagnetic Materials in Microwaves and Optics (Metamaterials '08) (Pamplona, Spain, Sep. 2008).
6. O. Sakai, T. Naito and K. Tachibana: “*Microplasma Array Serving as Photonic Crystals and Plasmon Chains* (Invited)”, International Congress on Plasma Physics (ICPP-2008) (Fukuoka, Japan, Sep. 2008).
7. T. Shirafuji, T. Morita, O. Sakai and K. Tachibana: “*Reaction Kinetics in the Plasma on the Water Surface*”, International Congress on Plasma Physics (ICPP-2008) (Fukuoka, Japan, Sep. 2008).

8. K. Urabe, Y. Ito, and K. Tachibana: “*Spatiotemporally Resolved Diagnostics of a Microplasma Jet Using Laser Spectroscopy Methods*”, International Congress on Plasma Physics (ICPP-2008) (Fukuoka, Japan, Sep. 2008) .
9. K. Tachibana: “*Microplasma Sources for Surface Engineering: Design and Characteristics* (Plenary)”, 11th International Conference on Plasma Surface Engineering (PSE-2008) (Garmisch-Partenkirchen, Germany, Sep. 2008).
10. D.-S. Lee, O. Sakai and K. Tachibana: “*Generation of Dynamic Metamaterial by Using Spoof Surface Plasmon on Patterned Silicon Substrate Assisted with Microplasma Array*”, 61st Annual Gaseous Electronics Conference (GEC2008) (Dallas, USA, Oct. 2008).
11. K. Tachibana: “*Generations, Characterizations and Applications of Microplasmas Operated in Atmospheric Gases and Artificial Media* (Invited)”, 55th International Symposium and Exhibition, American Vacuum Society (Boston, USA, Oct. 2008).
12. K. Tachibana: “*Microplasmas: Their Characteristics and New Applications* (Invited)”, 4th Vacuum and Surface Science Conference of Asia and Australia (VASSCAA-4), (Matsue, Oct. 2008).
13. M. Kawamoto, M. Nishitani, M. Kawasaki, Y. Yamamoto and K. Tachibana: “*Effect of a Pair of Annular Electrodes Buried in Barrier Ribs on Coplanar Discharge in an AC-PDP* (Best poster paper award)”, 15th International Display Workshops (IDW’08) (Niigata, Japan, Dec. 2008).
14. K. Tachibana: “*Discharge Plasma Phenomena in Gas-Liquid Composite Media and their New Applications* (Invited)”, IUMRS International Conference in Asia (Nagoya, Japan, Dec. 2008).
15. T. Shirafuji and K. Tachibana: “*Effects of Micro Bubbles on Pulse Discharge Characteristics in Water*”, IUMRS International Conference in Asia (Nagoya, Japan, Dec. 2008).
16. K. Tachibana: “*Microplasmas in Artificial Media: Generations and Applications* (Invited)”, Plasma Science Symposium 2009 / 26th Symposium on Plasma Processing (Nagoya, Japan, Feb. 2009).
17. K. Tachibana: “*Report on the Mext Consortium on Microplasmas in Japan from 2003 to 2008* (Invited)”, 5th International Workshop on Microplasmas (San Diego, CA, USA, Mar. 2009).
18. O. Sakai, T. Shimomura, D. -S. Lee and K. Tachibana: “*Metamaterials Activated by Microplasmas* (Invited)”, 5th International Workshop on Microplasmas (San Diego, CA, USA, Mar. 2009).
19. K. Urabe, Y. Ito and K. Tachibana: “*Investigation of Discharge Mechanisms in Microplasma Jet by Laser Spectroscopic Measurements*”, 5th International Workshop on Microplasmas (San Diego, CA, USA, Mar. 2009).
20. K. Tachibana: “*Efficient Generation of Microplasmas for Photonic and Processing Applications* (Invited)”, KAIST CAFDC International Workshop on Flexible Displays, Dejeon, Korea, Jun. 2009).
21. Y. Ito, Y. Fukui, K. Urabe and K. Tachibana: “*Study of Plasma Enhanced Chemical Vapor Deposition of Oxide Films by Non-thermal Plasma Jet at Atmospheric Pressure*”. 19th International Symposium on Plasma Chemistry (Bochum, Germany, Jul. 2009).
22. K. Tachibana: “*Microplasma Generation in Artificial Media and its Potential Applications* (Plenary)”, 19th International Symposium on Plasma Chemistry (Bochum, Germany, Jul. 2009).

23. K. Urabe, J. Choi, Y. Ito, K. Tachibana and O. Sakai: “*Diagnostics of Dielectric Barrier Discharges at Atmospheric Pressure by Laser Spectroscopic Measurements*”, 19th International Symposium on Plasma Chemistry (Bochum, Germany, Jul. 2009).
24. T. Morita, O. Sakai, T. Shirafuji and K. Tachibana: “*Underwater Chemical Reactions by Microplasmas inside Microbubbles Generated through Electrolysis*”, 19th International Symposium on Plasma Chemistry (Bochum, Germany, Jul. 2009).

4.2. Publications

25. O. Sakai, M. Kimura, T. Shirafuji and K. Tachibana: “*Underwater Microdischarge in Arranged Micro Bubbles Produced by Electrolysis in Electrolyte Solution Using Fabric-Type Electrode*”, Applied Physics Letters, Vol.93, No.23 (2008) pp.231501-1~3.
26. D.-S. Lee, K. Tachibana, H.-J. Yoon and H.-J. Lee: “*Enhancement of Optical Emission by Floating Electrodes in a Planar Microdischarge Cell*” Japanese Journal of Applied Physics, Vol.48, No.5 (2009) pp.056003-1~8.
27. D.-S. Lee, O. Sakai and K. Tachibana: “*Microplasma-Induced Deformation of an Anomalous Response Spectrum of Electromagnetic Waves Propagating along Periodically Perforated Metal Plates*”, Japanese Journal of Applied Physics Vol.48, No.6 (2009) pp.062004-1~7.
28. J.-Y. Choi, N. Takano, K. Urabe and K. Tachibana: “*Measurement of electron density in atmospheric pressure small-scale plasmas using CO₂-laser heterodyne interferometry*”, Plasma Sources Science and Technology, Vol.18, No. (2009) pp.035013-1~8.
29. K. Tachibana: “*Microplasma Processes at Atmospheric Pressure – Microplasma Sources for Local / Large-area Processing and their Potential Applications-*”, Journal of the Institute of Electrostatics Japan, Vol.33, No.3 (2009) pp.61-66, in Japanese.
30. D.-S. Lee, O. Sakai and K. Tachibana: “*Mode Change Observed on Spatial Distribution of Microplasma Emission in a Microdischarge Cell with a Floating Electrode*”, Japanese Journal of Applied Physics, Vol.48, No.10 (2009) in press.
31. K. Urabe, T. Morita, K. Tachibana and B. N. Ganguly: “*Investigation of Discharge Mechanisms in Helium Plasma Jet at Atmospheric Pressure by Laser Spectroscopic Measurements*”, under preparation for submission to Journal of Physics D: Applied Physics.
32. Y. Ito, Y. Fukui, K. Urabe, O. Sakai and K. Tachibana: “*Effect of Capacitance of Substrate on Accumulated Charge with Atmospheric Pressure Plasma Jet*”, under preparation for submission to Japanese Journal of Applied Physics.